Geo Statistics Term Paper:

Introduction and Motivation:

Through machine learning, we explore spatial and temporal aftershock patterns related to three instrumentally recorded earthquakes from eastern and central Idaho. Bordering the eastern extent of the Snake River Plain, within the Intermountain Seismic Belt of Idaho, we compare aftershock sequences related to the Sulphur Peak, Challis, and Stanley earthquakes. Upon implementing a machine learning algorithm to assist in the detection of seismic events, we are able to visualize where low magnitude events are occurring; therefore providing a robust temporal distribution of the aftershock sequences for each earthquake. The process of aftershock analysis for each sequence involved utilizing the aftershock catalogs obtained by the USGS and comparing the origin times, phase arrival, and depths to the same parameters obtained by an automated detection method. Through machine learning we increased the number of detected events from: 1,946 to 74,000 for the Stanley sequence, 189 to 7,079 for the Challis Sequence, and 551 to 2,916 for the Sulphur Sequence. The new aftershock catalog for Stanley witnessed the largest increase in catalog magnitude due to the dense array seismometers that were deployed temporarily near the epicentral zone of activity. Early aftershock analysis for Stanley ID, suggests that the extent of the Sawtooth Fault may extend farther than what is currently understood as results show a migration of events to the North-West extent of the currently mapped fault. The Challis sequence suggests similar preliminary results to the work of Pang and company in providing results that show a slight migration of event locations to the east and an increase in the average depth of events when compared to the USGS catalog. Preliminary results for Sulphur show an increase in depth estimates, with the majority of events occurring between 5-10km, as well as a migration of events to the north-west and south-east from the mainshock intersecting the normal faulting East-Bear lake fault. Despite increasing the magnitude of each sequence's seismic catalog a level of quality assurance is needed to assess the accuracy of the detected events. The assessment of our picks is determined by a measure of quality that relies on the origin times of detected events, phase arrivals, and distance of an event to the nearest station. A preliminary aftershock analysis for Stanley showed that phase time arrivals for P and S waves were on average less than half a second from those hand picked but moving forward with the other sequences there is variability in the quality of detected events for Challis and Sulphur. To assess the measure of quality obtainable using the machine learning algorithm the parameters for picking were manipulated. Assessing the detected events for the Challis Idaho Sequence provided picks of which 80% were poorly detected according to a relocation algorithm called Hypoinverse. This was not the case for the Sulphur or Stanley sequence. Therefore, by manipulating the picking thresholds and window size for similarity detection used by the automated detection algorithm a potential increase in the certainty of picks and phase detection could be obtainable. The significance of parameterizing the machine learning algorithm to work on a regional scale would allow seismologists to rely on automated detection algorithms for sequences that contain seismic events in close proximity to each other and in small time frame windows. Enhancing seismic detection for these sequences will aid our efforts in determining what role related faults play in future earthquakes and the driving mechanisms behind these three significant seismic events in Idaho.

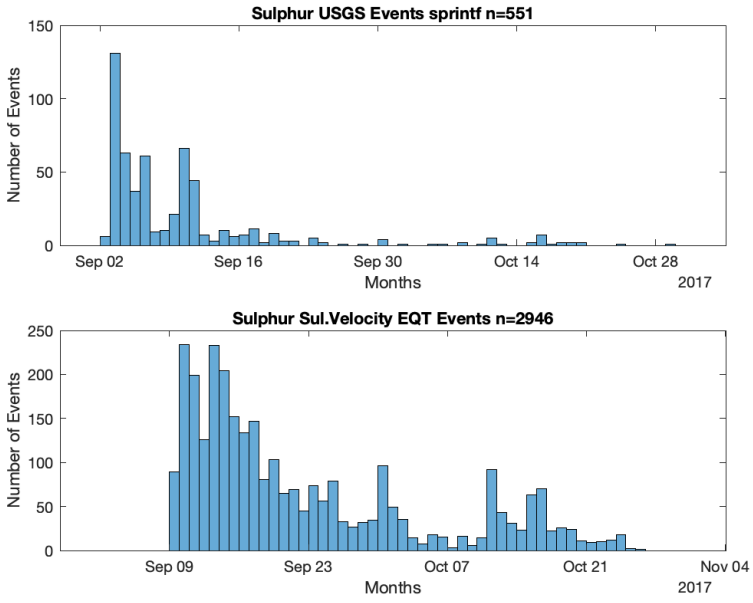

figure(1).a

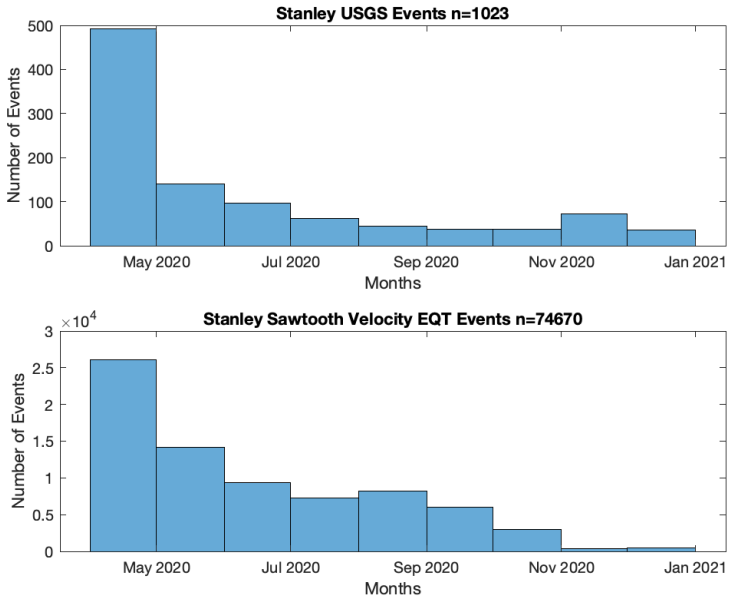

figure(1).b

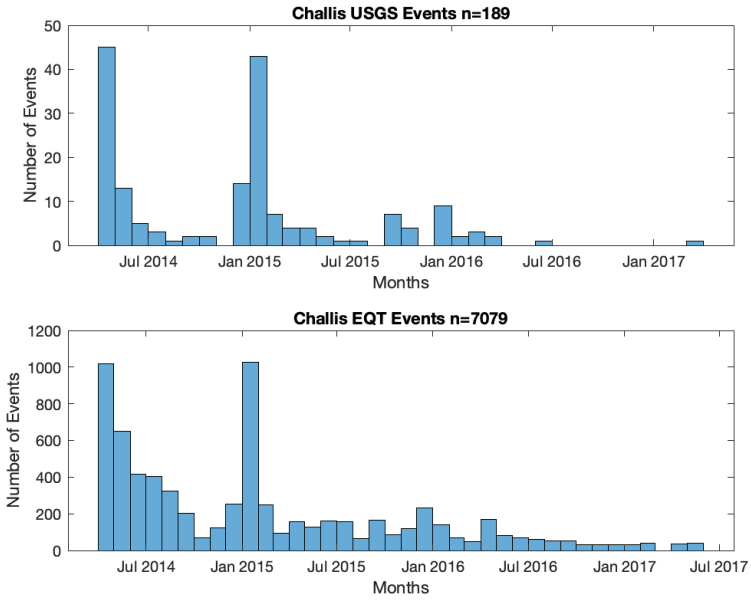

figure(1).c

Figure(1): Catalog comparison of detected events by EQTransformer compared to the machine learning catalog.

Methods:

To derive answers to the questions listed in the introduction regarding seismicity, I propose that by using an attentive deep learning model to detect and pick phases of aftershocks succeeding the mainshock, we may be able to better understand the cause of this event. Proceeding employment of the deep learning neural network we will need to assess the quality of the automated detection algorithms picks.

The event comparison is an essential step in determining the quality of our chosen machine learning algorithm and whether it will be a valuable tool in detecting low magnitude events and P and S wave phases for each event. The seismic data collected will consist of aftershocks of magnitude <M2.5. Rather than relying solely on a standard earthquake detection method, such as Short Term Average/Long Term Average (STA/LTA), which does not perform well when the signal to noise ratio is low, I plan to use an attentive deep learning algorithm that is not as limited by the signal to noise ratio. The new detection process is called EQTransformer. EQTransformer is a multi-task deep neural network that can be used for simultaneous earthquake detection and phase picking, while also treating each segment of continuous seismic data as a possible template for potential earthquakes (Mousavi & Ellsworth et al., 2020). This approach recognizes similarities in waveforms to an existing detected earthquake and uses this as a method to detect potential aftershocks. The process for identification can be broken down into two-levels of self attention, a global and local level; each level helps the program capture and exploit dependencies between local (individual phases) and global (full-waveform) features that are emitted from an earthquake signal (Mousavi & Ellsworth et al., 2020). The continuous data being fed to the algorithm are obtained using three-component seismometers. The data collected consists of north-to-south, east-to-west, and vertical components that provide the ground displacement at the sensor.

EQTransformer simultaneously detects events and picks the phase arrivals and using the output from EQTransformer we apply a relocation algorithm to relocate the event hypocenters using an appropriate

local velocity model. The relocation algorithm is called HYPOINVERSE and the output of the program is a .sum file that contains, latitude, longitude, travel time residuals, vertical/horizontal error, depth, origin time of the event, and a quality rating. The quality assessment is crucial in determining whether or not the location detected by EQT is an actual event and whether the phase arrivals are picked correctly on the waveform.

In order to assess the quality of the detected events from EQTransformer, Hypoinverse uses several parameters: root-mean-squared travel time residual (RMS) ERH (horizontal location error), ERZ (vertical location error), NWR number of weighted station reading phases, MAXGAP (maximum angular gap in degrees between azimuthally adjacent stations, the earthquake depth, and the minimum distance to the closest station. Using these parameters Hypoinverse applies a quality rating that is an average of two quality ratings.

The first quality rating is based on errors and goodness of fit.

A. RMS < 0.15 sec and ERH ≤ 1.0 km and ERZ ≤ 2.0 km
B. RMS <0.30 sec and ERH ≤ 2.5 km and ERZ ≤ 5.0 km
C. RMS < 0.50 sec and ERH $\leq$ 5.0 km
D. Worse than above

The second quality rating is based on station geometry:

A. NWR ≥ 6 and MAXGAP ≤ 90 and either DMIN $\leq$ DEPTH or DMIN ≤ 5.0
B. NWR ≥ 6 and MAXGAP ≤ 135 and either DMIN $\leq 2*$DEPTH or DMIN ≤ 10
C. NWR ≥ 6 and MAXGAP ≤ 180 and DMIN ≤ 50
D. Worse than above

The distance from the event to the earnest station is weighted using a krigging approach similar to what we learned in class. The ideal-distance weighting scheme allows for reducing the weight of the distant stations when an event is detected within the interior of a seismic network (Survey, G. 2002). The HYPOINVERSE distance weighting function is 1.0 for near stations and 0.0 for far stations and for those

in-between it follows a cosine taper.

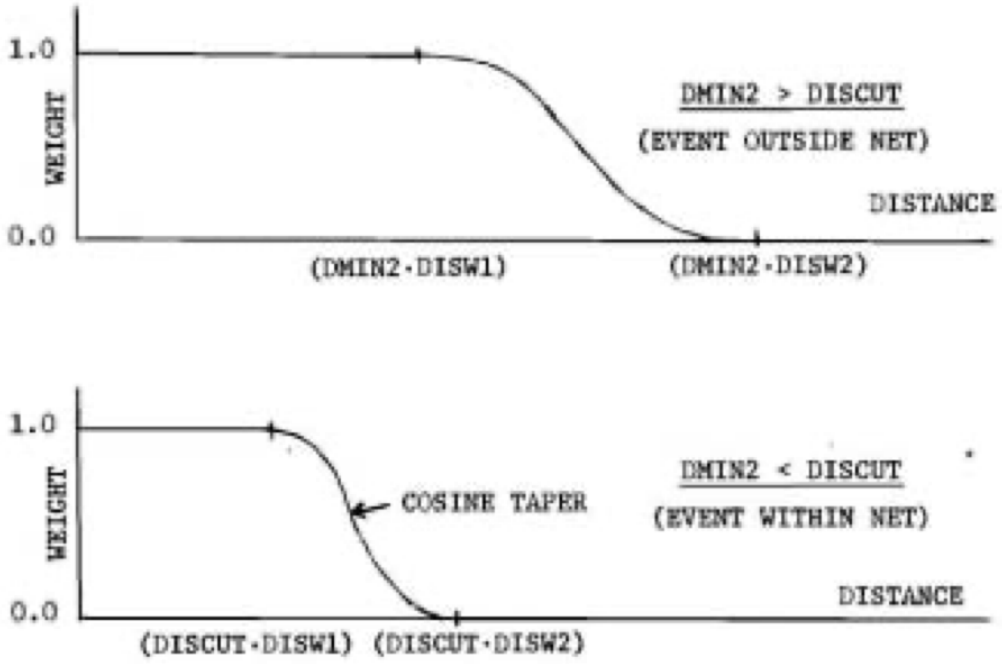

Figure (2). The distance weighting function as seen in the HYPOINVERSE Users Guide. .

DISCUT, DISW1 and DISW2 are constants set with the DIS command. DMIN2 is the distance to the second closest station. If DMIN2 is larger than DISCUT (upper figure), the function stretches out and scales with DMIN2 such that most of the network stations receive weights somewhere in the tapering part of the function. If DMIN2 is smaller than DISCUT (lower figure), the function is fixed. Stations farther than DISCUT x DISW2 then receive no weight. (Survey, G, 2002)

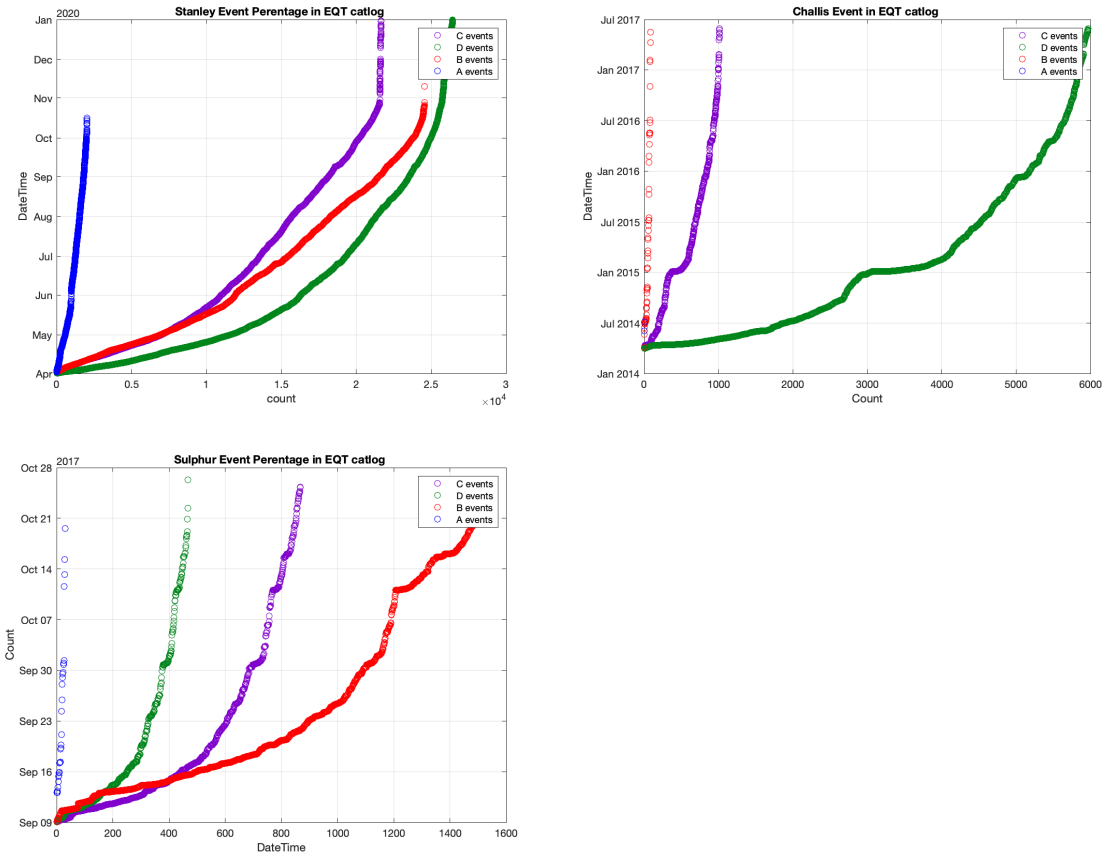

Figure(3). From top left to right: The number of quality events and the time they were detected for Stanley, Challis, and Sulphur in regards to the time of detection on the vertical axis.

To assist in determining the quality of the picks we dissected the parameters used in the weighting scheme for Hypoinverse. In doing so we came to the conclusion that "A" and "B" events are currently the most satisfactory based on the estimated travel time residuals and the depth of those events. We estimate from previous earthquake studies and the results of previous preliminary aftershock studies conducted by Pang 2018, Koper, 2019, and Liberty 2020, that any events occurring at depths greater than 20km have been poorly located. The majority of the "A" and "B" events for Stanley and Sulphur were within this estimated depth and this can be seen in the relative density histograms below.

Apart from determining what location events were desirable and which ones were poorly located, we wanted to determine if an appropriate local velocity model could constrain our earthquake locations even further. We did this by using the EQTransfromer picks and changing the velocity profile from the standard AK-135 model obtained from the IRIS database, to a local velocity model for the Stanley sequence from a developed 3-D isotropic crustal seismic velocity model of central Idaho and eastern Oregon passive seismic data (Bremner et al., 2019) was used and the Sulphur sequence was given the velocity model derived from a masters thesis completed by David Brumbaugh, 2001. By Comparing the local velocity model to the AK-135, we saw a decrease in the number of "A" and "B" picks because the standard deviation for each residual error was decreased. Despite having less "A" and "B" picks we were able to see with greater accuracy the hypocenters of the machine learning's tagged events. From this we can assume that some of the "C" picks that were further from a deployed seismic station may also contain events worth noting; but this will require further investigation regarding the nature of those events locations and the phase arrival times of the p and s waves to truly determine if we should include certain "C" quality events.

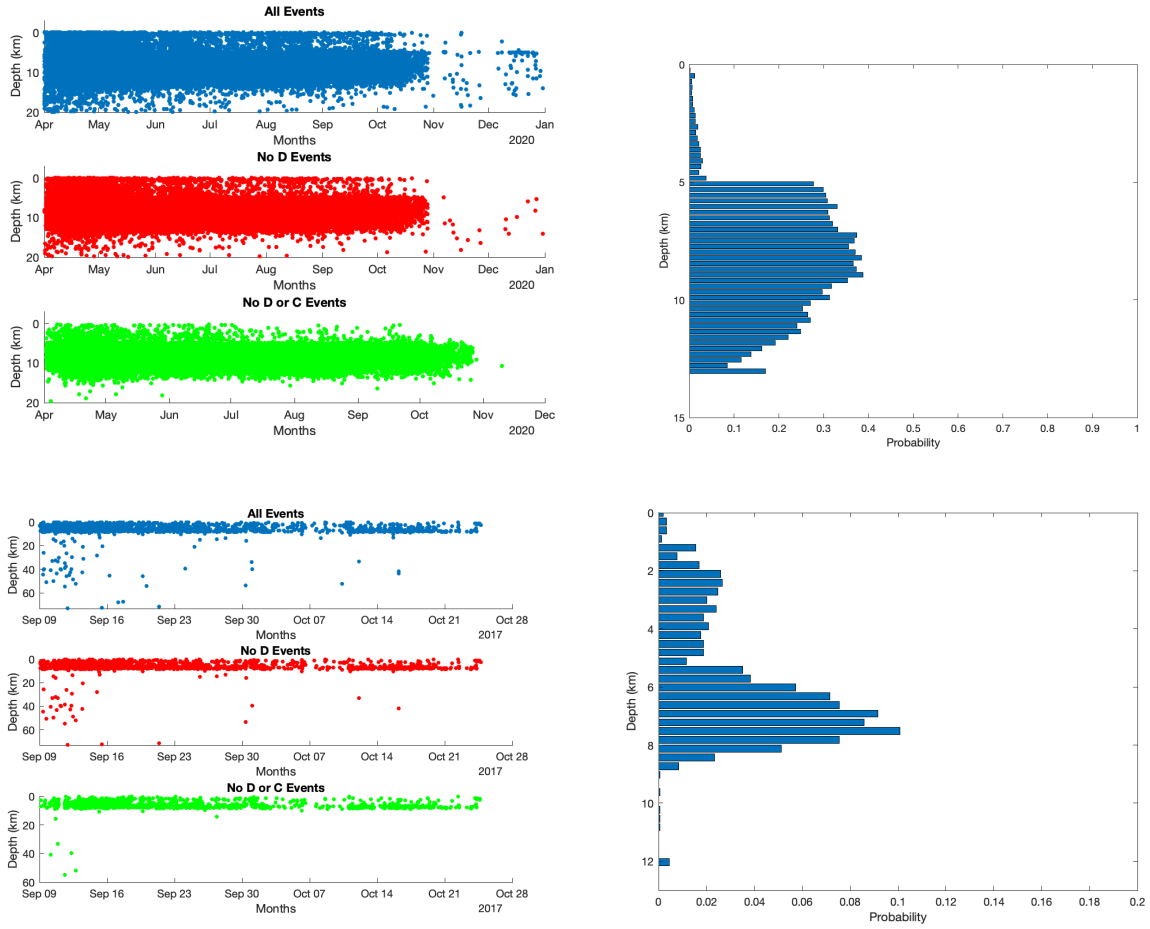

Figure (4). The depth plots above show the events for each sequence filtered by quality rating and then the histograms to the right show only the "A" and "B" events. The Stanley sequence shows that the majority of events are taking place somewhere between 8-10km in depth whereas the Sulphur sequence has a shallower active region of seismicity somewhere in between 6-8km in depth.

The plots above are only for the Sulphur and Stanley sequence due to the number of quality events and their respective residual error. TheChallis sequence is going to require further investigation and parameterized quality thresholds different from those set by HYPOINVERSE. The number of events that EQtransformer detected for Challis is 7079 as noted in figure (1c). While this is an impressive increase in the magnitude of our catalog we cannot confidently say all of those events are located with significant certainty. Using the preliminary results for Stanley and Sulphur we were able to get an idea of what residual errors we should expect for quality "A" and "B" events, using the depth, vertical, travel RMSE, and ignoring the station distance parameter we may be able to increase the number of significant events for the Challis sequence.

Appendix:

See linked files containing read_sum_function and the script Stanley_EQT_Events

References

Dewey, J. W. (1987). Instrumental Seismicity of Central Idaho *et a1., 1985). 1. June*, 819–836.

Crotwell, H. P., Owens, T. J., & Ritsema, J. (1999). *The TauP Too ~ kit : Flexib / e Seismic Travel-time and Ray-path Utilities*. *70*(April), 154–160.

Davenport, K. K., J. A. Hole, B. Tikoff, R. M. Russo, and S. H. Harder (2017). A strong contrast in crustal architecture from accreted terranes to craton, constrained by controlled-source seismic data in Idaho and eastern Oregon, Lithosphere 9, no. 2, 325–340.

Liberty, L. M., Lifton, Z. M., & Dylan Mikesell, T. (2021). The 31 March 2020 Mw 6.5 Stanley, Idaho, earthquake: Seismotectonics and preliminary aftershock analysis. *Seismological Research Letters*, *92*(2), 663–678. https://doi.org/10.1785/0220200319

Geiger, L. (1912). Probability method for the determination of earthquake epicenters from the arrival time only. Bulletin ofSaint Louis University, 8, 60–71

Kennett B.L.N., E.R. Engdahl and R. Buland. 1995. “Constraints on seismic velocities in the earth from travel times” Geophys. J. Int. 122, 108–124. https://doi.org/10.1111/j.1365-246X.1995.tb03540.x

Koper, K. D., Pankow, K. L., Pechmann, J. C., Hale, J. M., Burlacu, R., Yeck, W. L., Benz, H. M., Herrmann, R. B., Trugman, D. T., & Shearer, P. M. (2018). Afterslip Enhanced Aftershock Activity During the 2017 Earthquake Sequence Near Sulphur Peak, Idaho. *Geophysical Research Letters*, *45*(11), 5352–5361. https://doi.org/10.1029/2018GL078196

Mosher, S. G., & Audet, P. (2020). Automatic Detection and Location of Seismic Events From Time-Delay Projection Mapping and Neural Network Classification. *Journal of Geophysical Research: Solid Earth*, *125*(10), 1–18. https://doi.org/10.1029/2020JB019426

Mousavi, S. M., Ellsworth, W. L., Zhu, W., Chuang, L. Y., & Beroza, G. C. (2020). Earthquake transformer—an attentive deep-learning model for simultaneous earthquake detection and phase picking. *Nature Communications*, *11*(1). https://doi.org/10.1038/s41467-020-17591-w

Pang, G., Koper, K. D., Stickney, M. C., Pechmann, J. C., Burlacu, R., Pankow, K. L., Payne, S., & Benz, H. M. (2018). Seismicity in the Challis, Idaho, Region, January 2014-May 2017: Late aftershocks of the 1983 Ms 7.3 Borah Peak Earthquake. *Seismological Research Letters*, *89*(4), 1366–1378. https://doi.org/10.1785/0220180058

Payne, S. J., McCaffrey, R., & Kattenhorn, S. A. (2013). Extension-driven right-lateral shear in the centennial shear zone adjacent to the eastern snake river plain, Idaho. *Lithosphere*, *5*(4), 407–419. https://doi.org/10.1130/L200.1

Pollitz, F. F., Hammond, W. C., & Wicks, C. W. (2021). Rupture process of the M 6.5 Stanley, Idaho, earthquake inferred from seismic waveform and geodetic data. *Seismological Research Letters*, *92*(2 A), 699–709. https://doi.org/10.1785/0220200315

Stanciu, C. A., R. M. Russo, V. I. Mocanu, P. M. Bremner, S. Hongsresawat, M. E. Torpey, J. C. VanDecar, D. A. Foster, and J. A. Hole (2016). Crustal structure beneath the Blue Mountains terranes and cratonic North America, eastern Oregon, and Idaho, from teleseismic receiver functions, J. Geophys. Res., 121, 5049–5067

Survey, G. (2002). User's Guide to HYPOINVERSE-2000, a Fortran Program to Solve for Earthquake Locations and Magnitudes 4/2002.

Thackray, G. D., Rodgers, D. W., & Streutker, D. (2013). Holocene scarp on the sawtooth fault, central Idaho, USA, documented through lidar topographic analysis. *Geology*, *41*(6), 639–642. https://doi.org/10.1130/G34095.1

Trabant, C., A. R. Hutko, M. Bahavar, R. Karstens, T. Ahern, and R. Aster (2012), Data Products at the IRIS DMC: Stepping Stones for Research and Other Applications, Seismological Research Letters, 83(5), 846–854, https://doi.org/10.1785/0220120032.